

Electronic Supporting Information

Design and synthesis by ATRP of novel, water-insoluble, lineal copolymers and its application in the development of fluorescent and pH-sensing nanofibres made by electrospinning

Antonio L. Medina-Castillo*, Jorge F. Fernandez-Sanchez* Antonio Segura Carretero and Alberto Fernandez-Gutierrez

Department of Analytical Chemistry, University of Granada, Avd. Fuentenueva s/n, 18071 Granada, Spain. E-mail: antonioluismedina@ugr.es; jffernan@ugr.es

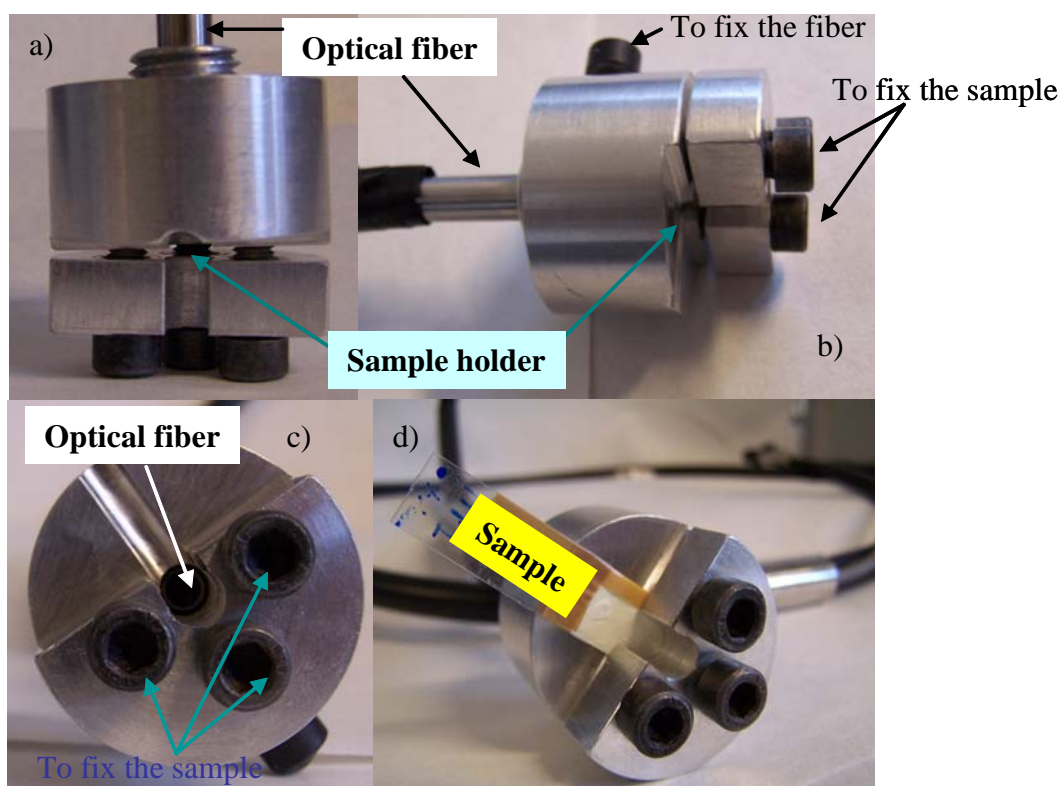


Fig. ESI-1. Several views of the home-made cell developed for the optical characterization of the pH-sensitive sensing films.

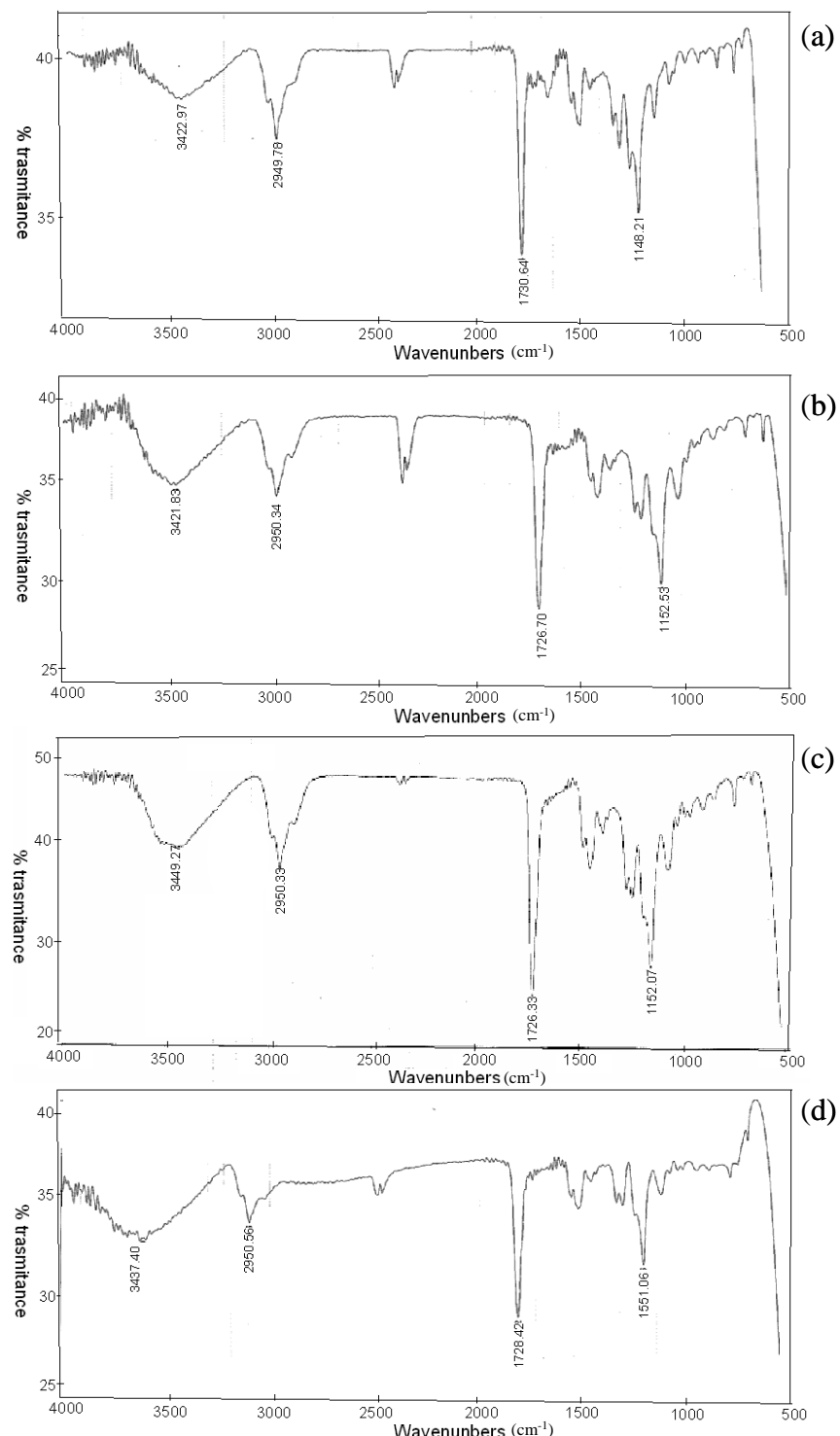


Fig. ESI-2. FT-IR spectra of a) NP0, b) NP1, c) NP1(X) and d) NP1(-)(A).

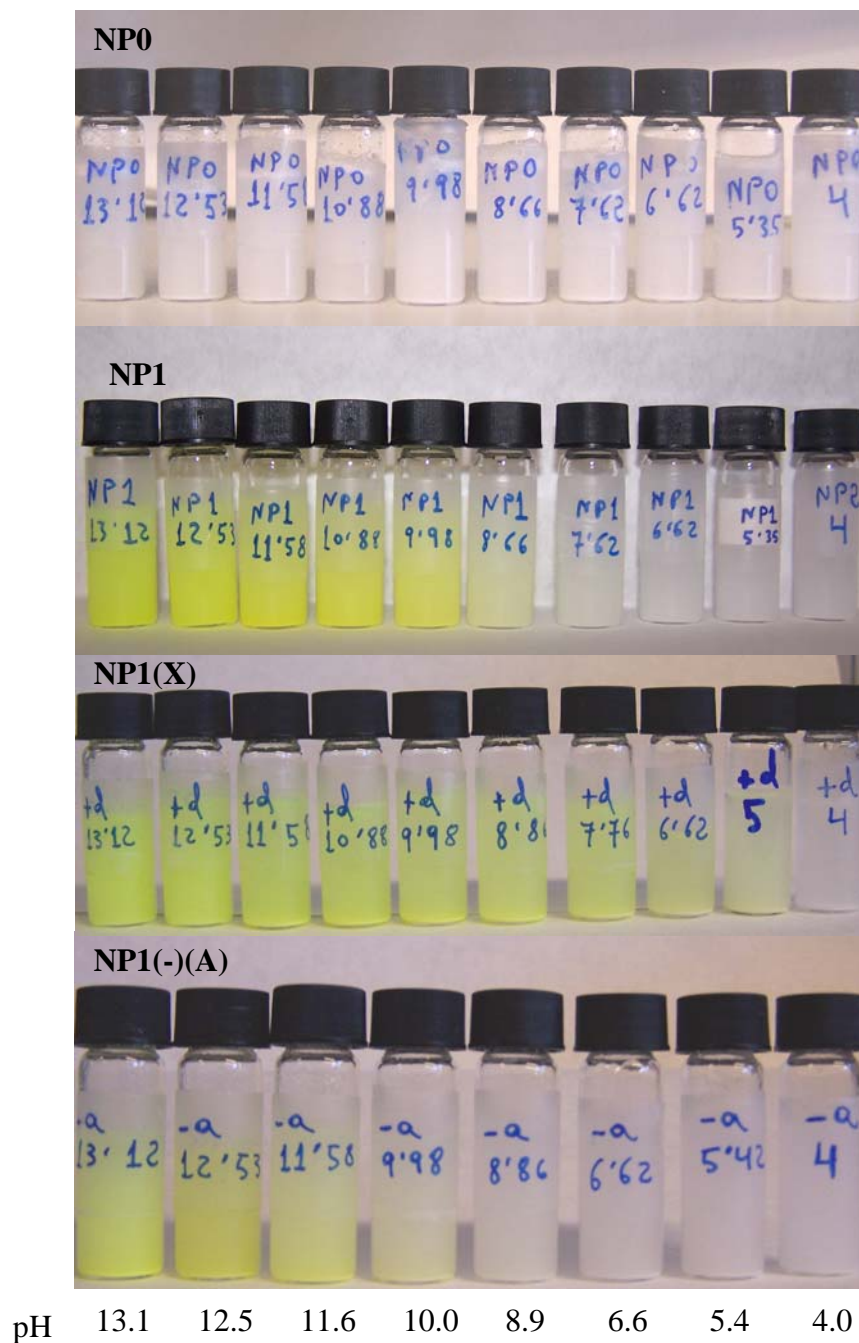


Fig. ESI-3. Pictures of the dispersions of NP0, NP1, NP1(X) and NP1(-)(A) in water at different pH values.

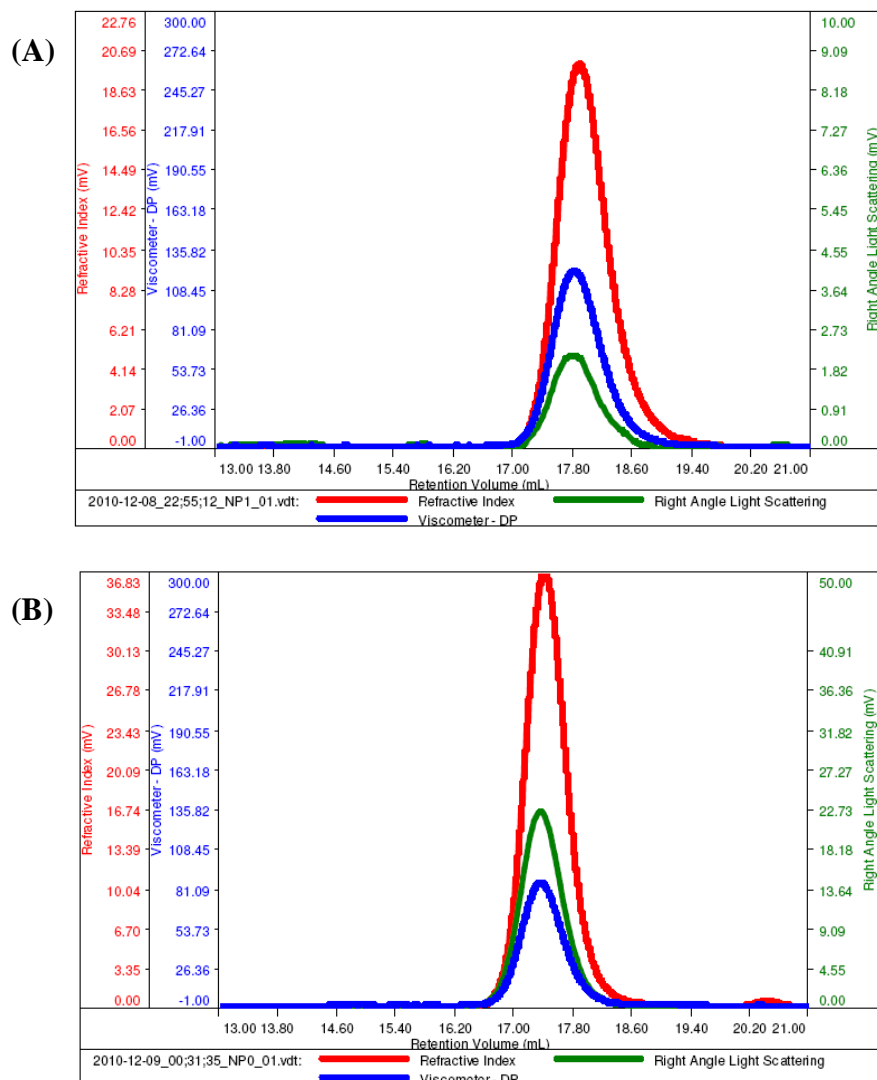


Fig. ESI-4 Triple detection GPC overlay of (A) NP1 and (B) NP0.

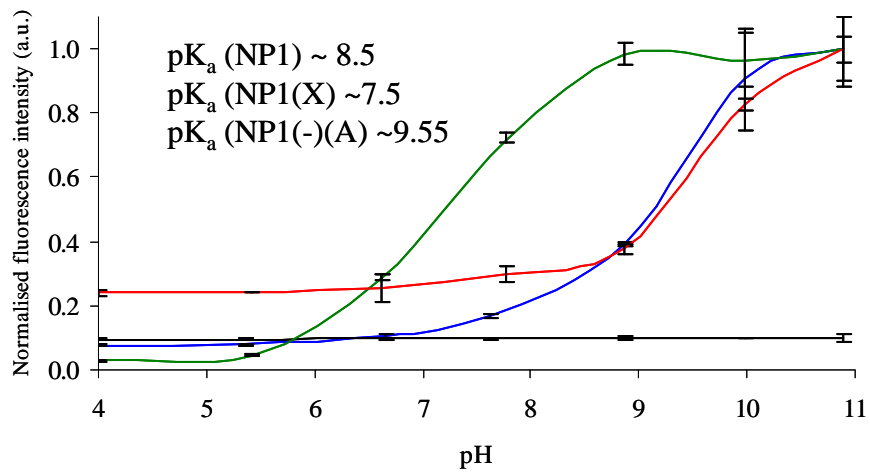


Fig. ESI-5. Comparison of the pK_a of the copolymers NP0 (—), NP1 (—), NP1(X) (—) and NP1(-)(A) (—).

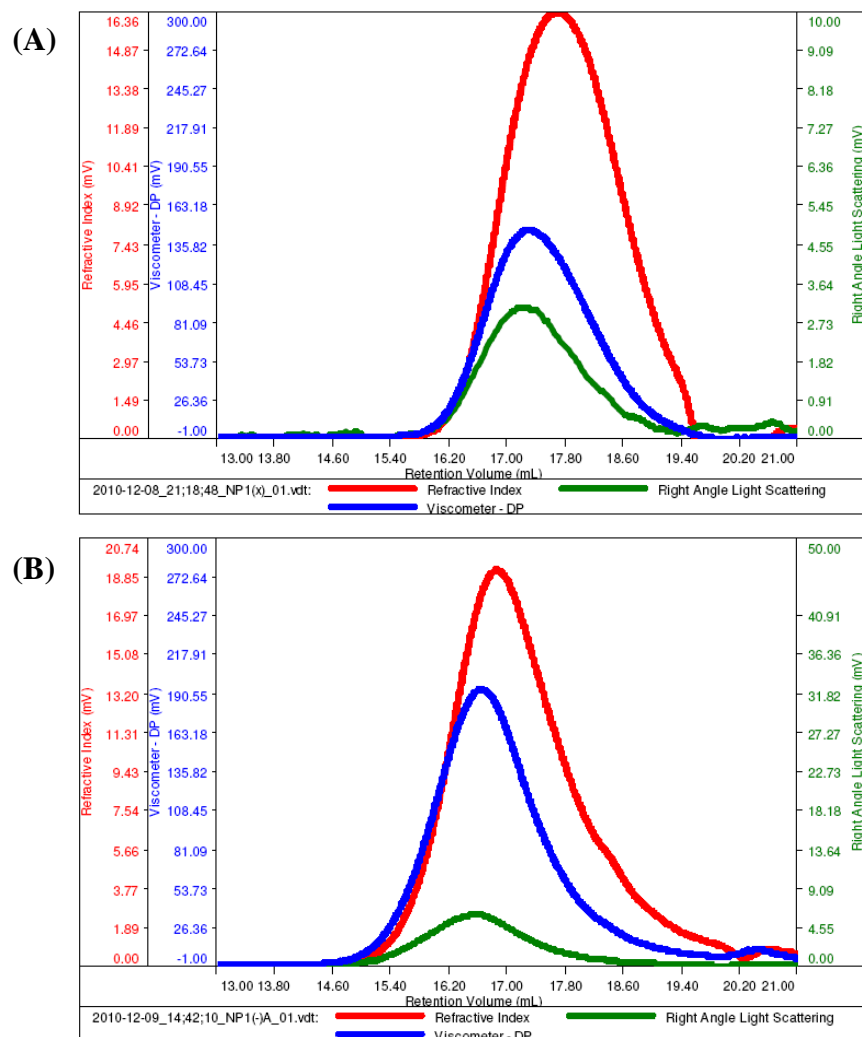


Fig. ESI-6 Triple detection GPC overlay of (A) NP1(X) and (B) NP1(-)(A).

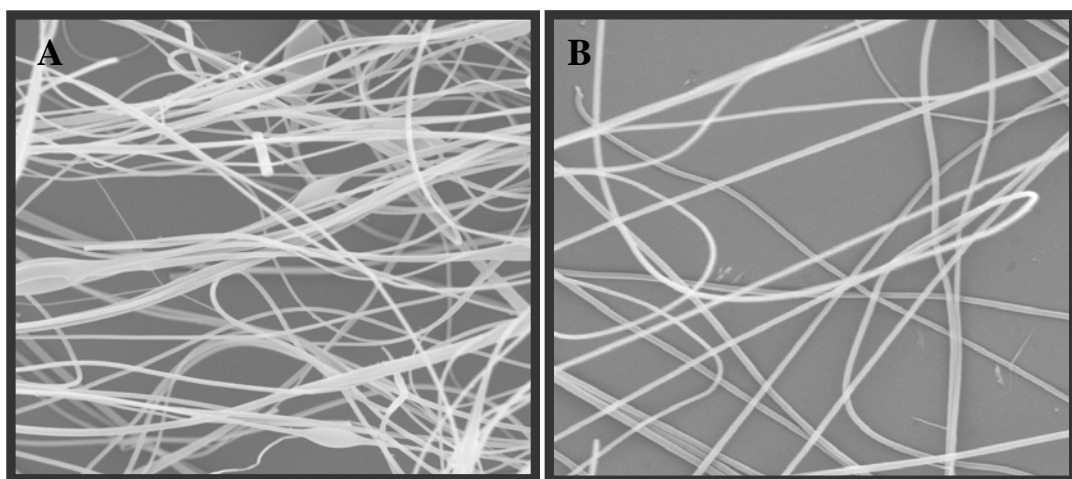


Fig. ESI-7 TEM picture of nanofibres prepared with A) low concentration of NP1 (20 wt %) and B) with high concentration of NP1 (40 wt %) and 1.75 wt % of HCl.

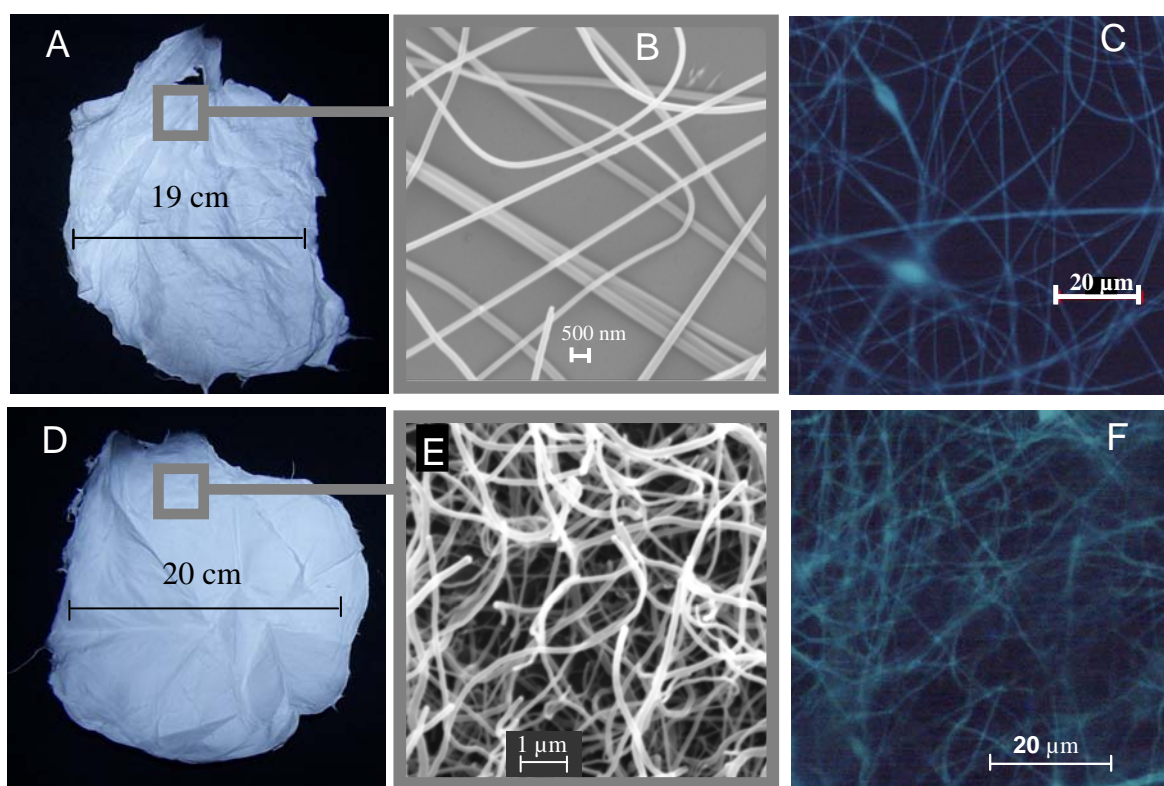


Fig. ESI-8. Figure 5 of the paper in colour.

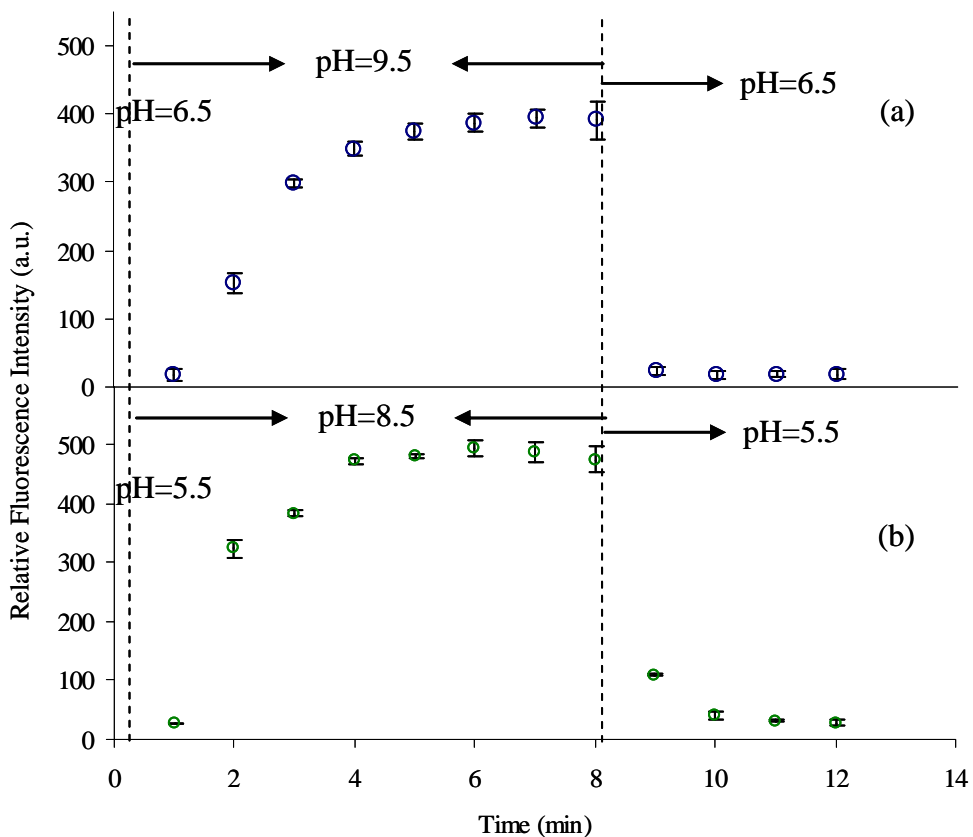


Fig. ESI-9. Determination of the equilibrium time of a) **N-F-NP1** and b) **N-F-NP1(X)** sensing films.

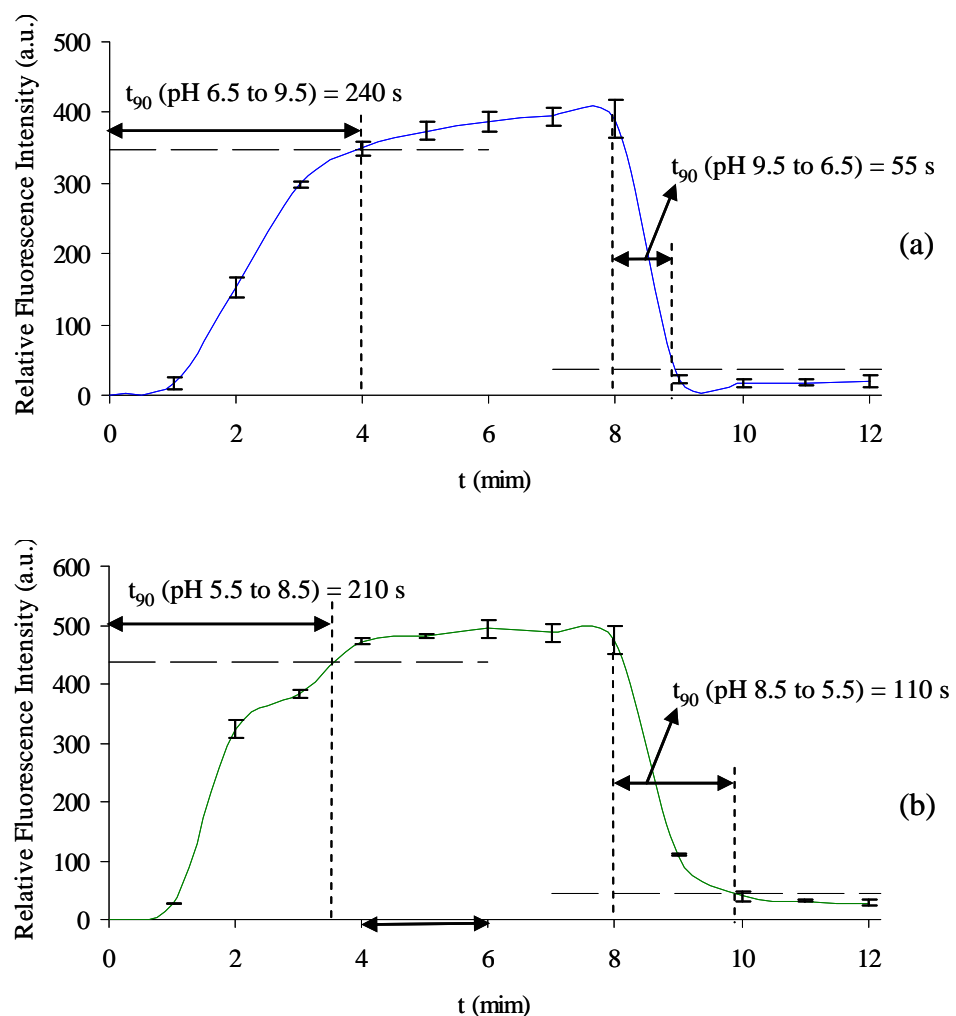


Fig. ESI-10. Determination of the t_{90} response time of a) F-N-NP1 and b) F-N-NP1(X) sensing films.

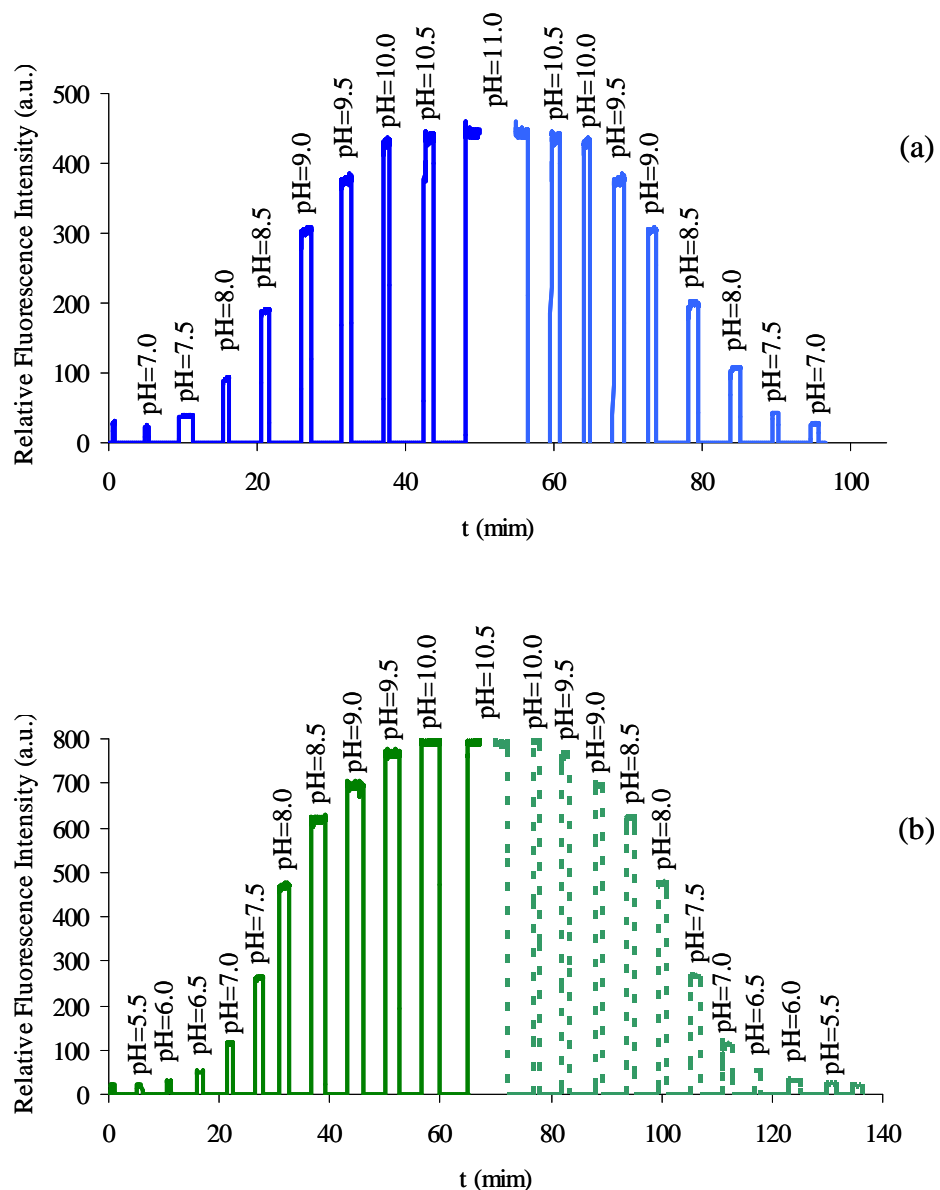


Fig. ESI-11. Reversibility of the sensing layers a) N-F-NP1 and b) N-F-NP1(X).